Determination of the three-dimensional orientation of single molecules

Matthew R. Foreman, Carlos Macías Romero, and Peter Török*

Blackett Laboratory, Department of Physics, Imperial College London, Prince Consort Road, London SW7 2BZ, UK
**Corresponding author: peter.torok@imperial.ac.uk*

Received February 1, 2008; accepted March 31, 2008;
posted April 3, 2008 (Doc. ID 92408); published April 30, 2008

A simple method for real-time determination of the full three-dimensional orientation of the emission dipole of single molecules is presented. Introduction of a π phase step in the back focal plane of the collector lens breaks the inherent symmetry, allowing the longitudinal dipole component to be measured. Experimental tolerances and the consequence of a nonzero bandwidth emission spectrum are also discussed. The scheme also allows for the longitudinal component of an electric field to be found experimentally. © 2008 Optical Society of America

OCIS codes: 180.2520, 260.2510, 300.2140.

Single-molecule detection and imaging techniques [1] have become important in recent years for studying dynamic processes such as chemical reactions and molecular motions, since information is not lost by the ensemble averaging typical of more traditional methods. Of particular interest is the determination of the orientation of the emission dipole of single molecules since it can be used as a means to label biological structures and track their conformational changes and motions [2]. Furthermore photophysical parameters of fluorophores, such as fluorescence lifetime, can depend on the molecule's orientation, a fact which can be used to study the molecule itself or its environment [3,4].

Many current techniques for determining the orientation of a dipole exist, e.g., [5,6]; however, these are limited to finding the transverse angle. Uncertainty over the longitudinal dipole component can lead to large errors (e.g., [3]), and hence it is desirable to find the full three-dimensional (3D) orientation of the molecule. Methods based on structured illumination, image fitting, and total internal reflection [7–9] can do this, although they are often restricted to specific circumstances, can be subject to a poor signal-to-noise ratio (SNR), and are not suitable for real-time measurements. In this Letter we present a novel technique capable of determining the 3D orientation of a single fluorescent molecule in real time. We then go on to consider the experimental tolerances associated with the setup including misalignments and the finite width of the molecule's emission spectrum.

We start by considering a fluorescent molecule as an electric dipole emitter with moment $\mathbf{p}=(p_x,p_y,p_z)$. A high NA lens is used collect and collimate the far-field radiation pattern. The lens is assumed to be ideal and immersed in a medium of the same refractive index as that containing the dipole. This constitutes a special case; however, a fuller treatment in which the dipole field propagates through dielectric interfaces (e.g., a coverglass–immersion fluid interface) does not alter the symmetry of the problem [10] and hence the following discussion is unchanged.

Vectorial ray tracing can be used to find the electric field $\mathbf{E}_{bf}$ in the back focal plane of the collector lens by using generalized Jones matrices. This yields [11]

$$\mathbf{E}_{bf}=\frac{1}{2\sqrt{\cos\theta}}\begin{pmatrix} p_x a_1^x - p_y a^y - 2p_z a_1^z \\ p_y a_2^x - p_x a^y - 2p_z a_2^z \\ 0 \end{pmatrix}, \tag{1}$$

where

$$a_1^x=(1+\cos\theta)-(1-\cos\theta)\cos 2\phi,$$

$$a_2^x=(1+\cos\theta)+(1-\cos\theta)\cos 2\phi,$$

$$a^y=(1-\cos\theta)\sin 2\phi,$$

$$a_1^z=2\sin\theta\cos\phi,$$

$$a_2^z=2\sin\theta\sin\phi. \tag{2}$$

The $\sqrt{\cos\theta}$ factor is required to ensure energy conservation [12].

Equation (1) shows that we can consider the field in the back focal plane as having contributions from three independent electric dipoles aligned with the coordinate axes. The field distributions associated with each of these dipoles are shown in Fig. 1.

Refocusing of the collected beam by a second lens corresponds to a coherent integration over the back focal plane. The symmetry of the distributions in Fig. 1 immediately shows that points in the integration plane will either cancel pairwise or superpose constructively. The resulting field at the focus thus takes the form $\mathbf{E}_f \propto (p_x,p_y,0)$, where the z component is negligible since we refocus with a low NA lens. This can also be shown rigorously by integration of Eq. (1). Refocusing by a high NA lens, as described by the Debye–Wolf diffraction integral [13], gives a similar result whereby $\mathbf{E}_f \propto (K_1 p_x, K_1 p_y, K_2 p_z)$ at the focus, where K_1 and K_2 are constants and $K_2/K_1 \ll 1$ [11].

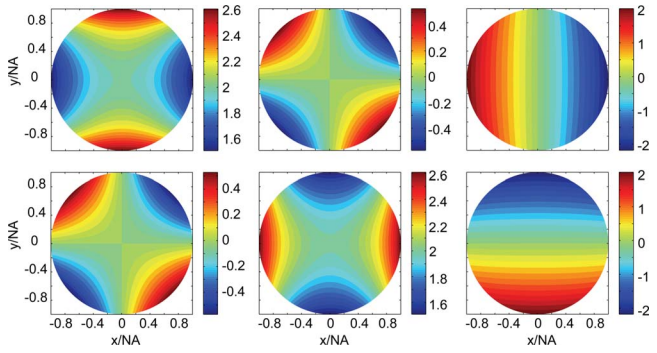

Fig. 1. (Color online) Field distributions for E_x (top) and E_y (bottom) in the back focal plane of a collecting lens (NA=0.966) arising from orthogonal electric dipoles orientated along the x, y, and z coordinate axes (left to right).

This result encapsulates the difficulty in determining the p_z component of a dipole; however, it also suggests a means by which it can be overcome. A significant p_z dependence can be introduced into the "image" of the dipole by breaking the symmetry of the distributions in the back focal plane of the collector lens. This could be done, for example, by apodization or phase modification of the beam. We elect to consider the latter since it does not inherently reduce the optical throughput of the system, which is a major issue in single molecule experiments [14]. We hence propose the optical setup shown in Fig. 2 as a means to detect the full 3D orientation of an electric dipole in real time.

Light collected from the dipole is incident into a beam splitter from which one of the output beams is further passed through a Wollaston prism (WP), which splits the field into its constituent x and y components. The other portion of light output from the beam splitter is passed through a phase mask that imposes a π phase delay to the beam in the first and fourth quadrants with respect to the beam in the second and third quadrants so as to break the symmetry as discussed above. The mask (shown in Fig. 3) thus has an amplitude transmittance function of

$$T(x,y) = \begin{cases} -1 & \text{for } x \geq 0 \\ +1 & \text{for } x < 0 \end{cases}. \tag{3}$$

In its simplest form this could be implemented using

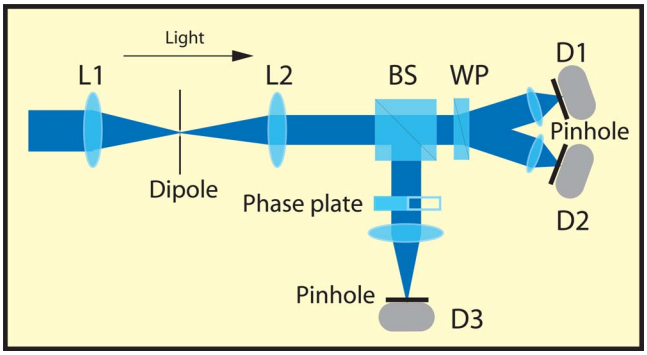

Fig. 2. (Color online) Proposed optical setup for determination of the full 3D orientation of an electric dipole.

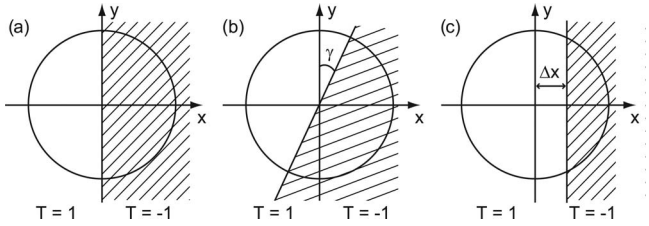

Fig. 3. (a) Proposed phase mask. (b) Rotational misalignment. (c) Translational misalignment.

a glass block of appropriate thickness placed across one half of the beam.

Finally the field in each arm is refocused onto point detectors (such as avalanche photodiodes) D_1, D_2, and D_3, so that detection is field sensitive, yielding measurements of $C_x|p_x|^2$, $C_y|p_y|^2$, and $C_z|p_z|^2$, respectively. It is reasonable to assume that $C_x=C_y$ since the two detection arms are identical albeit for a 90° rotation in the state of polarization. We note that introduction of an additional arm with a polarizer at 45° to the x axis allows the angular ambiguity as to which quadrant the dipole lies in to be removed, although the light incident on each detector is reduced. Furthermore the magnitude of the dipole components for a general dipole will depend on the excitation field, which then has consequences for the SNR in each detector. The illumination must hence be matched to the specific detection needs.

For orientational measurements it is necessary to work with only the ratios between the detector signals. The value of the constant $C=C_x/C_z$ must be found by means of a calibration scan of a free dipole, which can be physically realized using point scatterers [15]. We note that C is dependent on the splitting ratio of the beam splitter and can hence be controlled to some extent but does cause a trade-off of SNR between different detector arms. Since the scatterer reradiates as a dipole with an effective moment $\mathbf{p}_{\text{eff}} \propto \mathbf{E}_{\text{ill}}$, the three detector signals will theoretically map the focused field distribution, which can be calculated exactly using the Debye–Wolf integral. It is then a simple matter to determine the constant of proportionality. This method hence also provides a means to measure the longitudinal component of an electric field distribution.

Of importance in any practical implementation of the proposed detection scheme are the alignment tolerances of the phase mask. We consider both rotational and translational misalignments of the mask as depicted in Fig. 3, since any misalignment can be treated as a combination of both. A rotational misalignment by an angle γ modifies the transmittance function. However, assuming a symmetric pupil (which is normally the case) integration over the field does not yield any dependence on γ. The detector signals are thus insensitive to pure rotational misalignments, a property that can again be attributed to the symmetrical nature of the back focal plane field distributions.

Translational misalignments of the mask do however have a detrimental effect on the detector signals. A horizontal shift of Δx modifies the transmittance function to

$$T(x,y) = \begin{cases} -1 & \text{for } x \geq \Delta x \\ +1 & \text{for } x < \Delta x' \end{cases} \quad (4)$$

which in general causes a mixing of the p_x and p_y signals into D_3. Figure 4 shows the degree to which this affects the system, as found by numerical simulations and as parameterized by the extinction ratios between the measured signal in D_3 for a pure x and y dipole (denoted D_3^x and D_3^y, respectively) relative to that for a pure z dipole (D_3^z).

Hitherto discussion has been limited to monochromatic light of wavelength λ. This is however an unrealistic assumption, since fluorescent molecules emit a spectrum $S(\lambda)$ of wavelengths of bandwidth $\Delta\lambda$. A nonzero bandwidth will have consequences with regard to the glass slab used to impose the π phase delay, since it can only be designed to operate perfectly at a single wavelength. The signal recorded in each detector can be calculated using

$$D_\nu^{\text{tot}} = \int_{\lambda_{\min}}^{\lambda_{\min}+\Delta\lambda} S(\lambda) D_\nu(\lambda) d\lambda \quad \nu = 1,2,3, \quad (5)$$

where $D_\nu(\lambda)$ is the detector reading for light of wavelength λ in the presence of a phase plate designed for operation at λ_0 and $\lambda_{\min}$ is the lower bound on the spectrum.

Results from numerical simulations assuming a Lorentzian spectrum profile centered on $\lambda_0 = 450$ nm are shown in Fig. 4(a). Other spectral profiles give similar results. Only the extinction ratios for D_3 are shown since no variation is seen in D_1 and D_2. We see that the p_x and p_y signals mix into the D_3 signal and become double that of the p_z measurement for a bandwidth of $\sim$100 nm. Although typical fluorophores have bandwidths of approximately 30 nm, this mixing effect can limit the performance of the setup. Use of broadband wave plates to implement the phase mask can however greatly improve the situation.

As a final consideration we relax the previous assertion of point detectors. In general D_1 and D_2 operate as confocal microscopes with finite-sized pinholes illuminated with x and y polarized light, respectively, an analysis of which can be found in [16]. Thus here we only consider measuring a pure p_z dipole. It is found that the SNR arising in this case is worse than for measuring pure p_x and p_y dipoles and is hence the limiting case.

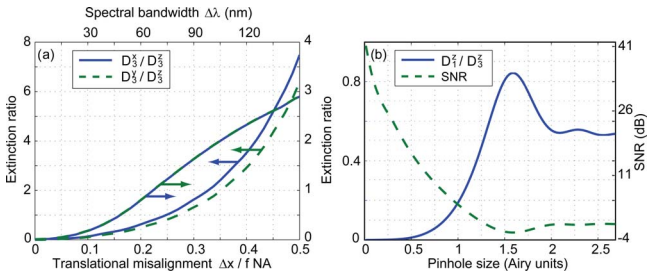

Fig. 4. (Color online) (a) Extinction ratios as a mask misalignment (bottom-left axes) and spectral bandwidth (top-right axes). (b) SNR for finite detector sizes.

Finite-sized detectors record the integrated intensity of the focused light distribution over their extent; however, when imaging a dipole the off-axis intensity is dependent on all three dipole components [11]. For a dipole with moment $\mathbf{p} = (0,0,1)$ parasitic signals are thus introduced into D_1 and D_2. Treating these signals as noise, the SNR can be defined as $10 \log_{10}(D_3^z / 2D_1^z)$, the behavior of which is shown in Fig. 4(b) along with that of the extinction ratio $D_1^z/D_3^z = D_2^z/D_3^z$. Typical values of the SNR in single molecule experiments are $\sim$15 dB [14]. As such, Fig. 4(b) shows that the effect of a finite detector size becomes more dominant once the radius of the detector is approximately half the size of the Airy disk. Detectors smaller than this are thus preferable.

In summary we have found that by breaking the symmetry of the back focal plane field distributions from an imaged electric dipole it is possible to determine the longitudinal component of its dipole moment. More specifically a scheme whereby one half of the collected beam is subject to a π phase delay has been presented. Potential sources of error for experimental implementations have also been discussed. Future work in this field is to include experimental verification of the principles of operation of the method. We finally note that the discussed technique works equally well when imaging the electric field of magnetic dipoles.

References

1. W. E. Moerner and D. P. Fromm, Rev. Sci. Instrum. **74**, 3597 (2003).
2. S. Weiss, Nat. Struct. Biol. **7**, 724 (2000).
3. T. Ha, T. Enderle, D. F. Ogletree, D. S. Chemla, P. R. Selvin, and S. Weiss, Proc. Natl. Acad. Sci. USA **93**, 6264 (1996).
4. L. A. Deschenes and D. A. Van den Bout, Science **292**, 233 (2001).
5. T. Ha, T. Enderle, D. S. Chemla, P. R. Selvin, and S. Weiss, Phys. Rev. Lett. **77**, 3979 (1996).
6. T. M. Jovin, M. Bartholdi, W. L. C. Vaz, and R. H. Austin, Ann. N.Y. Acad. Sci. **366**, 176 (1981).
7. B. Sick, B. Hecht, and L. Novotny, Phys. Rev. Lett. **85**, 4482 (2000).
8. R. M. Dickson, D. J. Norris, and W. E. Moerner, Phys. Rev. Lett. **81**, 5322 (1998).
9. D. Patra, I. Gregor, and J. Enderlein, J. Phys. Chem. A **108**, 6836 (2004).
10. P. Török, Opt. Lett. **25**, 1463 (2000).
11. P. Török, P. D. Higdon, and T. Wilson, J. Mod. Opt. **45**, 1681 (1998).
12. D. J. Innes and A. L. Bloom, Spectra-Phys. Laser Tech. Bull. **5**, 1 (1966).
13. B. Richards and E. Wolf, Proc. R. Soc. London, Ser. A **253**, 358 (1959).
14. M. R. Foreman, S. S. Sherif, and P. Török, Opt. Express **15**, 13597 (2007).
15. H. C. van de Hulst, *Light Scattering by Small Particles* (Dover, 1981).
16. P. Török, P. D. Higdon, and T. Wilson, Opt. Commun. **148**, 300 (1998).